Title

Steady-state junction current distribution in p-n GaN diodes measured using low-energy electron microscopy (LEEM)

Journal

Applied Physics Letters, 123(3)

ISSN

0003-6951

Authors

Ho, Wan Ying

Johnson, Cameron W

Tak, Tanay

et al.

Publication Date

2023-07-17

DOI

10.1063/5.0153947

Peer reviewed

Applied Physics Letters

RESEARCH ARTICLE | JULY 17 2023

Steady-state junction current distribution in p-n GaN diodes measured using low-energy electron microscopy (LEEM)

Wan Ying Ho ; Cameron W. Johnson; Tanay Tak ; Mylène Sauty ; Yi Chao Chow ; Shuji Nakamura ; Andreas Schmid ; Jacques Peretti ; Claude Weisbuch ; James S. Speck

Appl. Phys. Lett. 123, 031101 (2023)
https://doi.org/10.1063/5.0153947

Applied Physics Letters ARTICLE pubs.aip.org/aip/apl

Steady-state junction current distribution in p-n GaN diodes measured using low-energy electron microscopy (LEEM)

Cite as: Appl. Phys. Lett. **123**, 031101 (2023); doi: 10.1063/5.0153947
Submitted: 12 April 2023 · Accepted: 4 July 2023 ·
Published Online: 17 July 2023

View Online Export Citation CrossMark

Wan Ying Ho,[1,a)] Cameron W. Johnson,[2] Tanay Tak,[1] Mylène Sauty,[3] Yi Chao Chow,[1] Shuji Nakamura,[1,4] Andreas Schmid,[2] Jacques Peretti,[3] Claude Weisbuch,[1,3] and James S. Speck[1]

AFFILIATIONS

[1]Materials Department, University of California, Santa Barbara, California 93106-5050, USA
[2]Molecular Foundry, Lawrence Berkeley National Laboratory, One Cyclotron Road, Building 67, Berkeley, California 94720, USA
[3]Laboratoire de Physique de la Matière Condensée, CNRS, Ecole Polytechnique, IP Paris, 91120 Palaiseau, France
[4]Department of Electrical Engineering, University of California, Santa Barbara, California 93106-5050, USA

[a)]**Author to whom correspondence should be addressed:** wanying_ho@ucsb.edu

ABSTRACT

We report on the measurement of the lateral distribution of the junction current of an electrical biased *p-n* GaN diode by electron emission microscopy using a low-energy electron microscope. The vacuum level at the surface of the diode was lowered by deposition of cesium to achieve negative electron affinity, allowing overflow electrons at the surface of the biased diodes to be emitted and their spatial distribution imaged. The results were compared to the literature, and a good match with analytical solutions by Joyce and Wemple [J. Appl. Phys. **41**, 3818 (1970)] was obtained.

In III-nitrides, due to the necessity to use insulating sapphire substrates, a typical light-emitting diode (LED) mesa structure involves open apertures contacted by a *p*-contact side-by-side with the *n*-contact, forming a combination of vertical and lateral current flows. The lateral current flow in a diode is highly non-linear, with current crowding near the metal edges leading to non-uniform emission and local heating effects.[1–6] At visible wavelengths, these issues can be reasonably mitigated by employing transparent conductive oxides (TCOs), which introduces light absorbers and cannot be extended to other wavelengths.[7] It is, hence, important to study the potential and steady-state current profile of a diode design, as they inform current crowding circumvention in LEDs and laser diodes.

For a resistive p-doped semiconductor contacted to a highly conductive n-layer, the local junction current density $J(\vec{r})$ follows the ideal diode equation, i.e.,

$$J(\vec{r}) = J_S\Big(\exp\left[\beta V(\vec{r})\right] - 1\Big), \tag{1}$$

$$\approx J_S \exp\left[\beta V(\vec{r})\right], \tag{2}$$

where $\vec{r}$ is the distance from the metal contact, J_S is the reverse-bias saturated junction current density, V is the potential, $\beta = q/\eta k_B T$, η is the ideality factor of the diode, T is the temperature, q is the fundamental charge, and k_B is the Boltzmann constant. The approximation in Eq. (2) is valid under typical forward bias operation. Using Ohm's Law, the lateral film current density C for a resistive thin film with sheet resistance R_S is

$$\nabla V(\vec{r}) = -R_S C(\vec{r}). \tag{3}$$

For simplicity, without loss of generality, the potential of the *n*-layer is taken to be grounded. Since the only way current can leave the *p*-layer is through the junction, we have

$$\nabla \cdot C(\vec{r}) = J(\vec{r}). \tag{4}$$

Hence, taking the divergence of Eq. (3) yields

$$\nabla \cdot C(\vec{r}) = \frac{1}{R_S}\nabla^2 V(\vec{r}) = J_S \exp\left[\beta V(\vec{r})\right] = J(\vec{r}). \tag{5}$$

Joyce and Wemple solved Eq. (5) for circular apertures contacted at the edge as depicted in Fig. 1, where a highly resistive *p*-region (*p*-GaN) forms a *p-n* junction with the highly conductive *n*-region (*n*-GaN).[1] The junction current changes radially from the metal contact as described by the following solution:

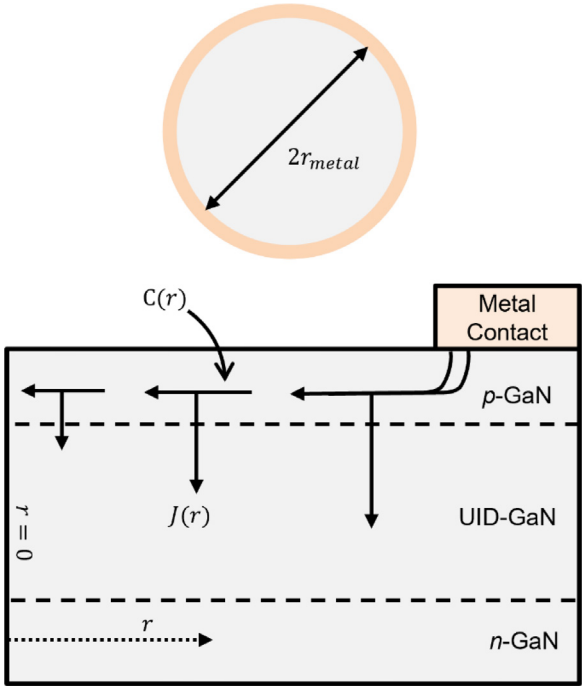

FIG. 1. Schematic of the device solved analytically in Ref. 1, which is of experimental interest in this work. A circular aperture with center at $r = 0$ is contacted at the edge at radius r_{metal} by an annular metal contact of finite width.

$$J(\vec{r}) = J_{metal}\left(1 - \frac{I_{aper}\beta R_S}{8\pi}\left[1 - \frac{r^2}{r_{metal}^2}\right]\right)^{-2}. \quad (6)$$

I_{aper} is the *total* current flowing outward from the circular aperture, i.e., it represents the total current supplied to the open circular aperture.[1] Since all the lateral current in p-GaN leaves the layer through the junction, we have

$$I_{aper} = \int_0^{r_{metal}} 2\pi \cdot J(r)dr. \quad (7)$$

In an experiment measuring the optical emission from an LED, Guo and Schubert compared their results to a *lateral* current transport model.[2] They found that the current from the p-contact metal edge to the n-contact in the lateral device can be described using an exponential decay model:

$$J(r) = J_{metal}\exp\left(-\frac{x}{L_S}\right), \quad (8)$$

where $L_S = \sqrt{(\rho_c + \rho_p t_p)t_n/\rho_n}$ is the current spreading length, ρ_c is the specific contact resistivity of the p-contact, $x = r_{metal} - r$ is the distance from the metal contact, while $t_p(t_n)$ and $\rho_p(\rho_n)$ are the thickness and resistivity of the p-layer (n-layer). This model was later modified to include lateral current flow in p-GaAs by Rattier *et al.*, where $L_S = \sqrt{2\eta k_B T/[q(R_{s,p} + R_{s,n})J_{metal}]}$.[5,8,9] Interestingly, while Guo and Schubert obtained good agreement between the exponential decay model and their optical emission distribution, a similar experiment performed using spatially resolved photocurrent measurements showed a slight disagreement further away from the contact metal.[2,5] In the work by Meriggi *et al.*, a square grid metal contact was employed instead; thus, the lateral device model may not be as suitable.[5]

In this Letter, we report on experimental verification of the steady-state current profile of a p-n GaN diode using electron emission microscopy (EEM) and we compared the results to the calculations of Joyce and Wemple. EEM was performed in an Elmitec LEEM III Low Energy Electron Microscope at the Molecular Foundry of the Lawrence Berkeley National Laboratory, which will be described later. The GaN diode was grown by metalorganic chemical vapor deposition (MOCVD) on flat sapphire, with 2 μm of n-GaN ([Si]$= 4.0 \times 10^{18}$ cm^{-3}), 1 μm of unintentionally doped (UID) GaN, and 200 nm of p-GaN ([Mg]$= 3.5 \times 10^{19}$ cm^{-3}) and capped with 15 nm of highly doped p-GaN ([Mg]$= 2.0 \times 10^{20}$ cm^{-3}). The doping was measured using secondary ion mass spectroscopy (SIMS).

The diode was formed by a Pd/Au (5/25 nm) p-contact with an open circular aperture lithographically defined with known radius of 80, 20, 10, and 5 μm [see Fig. 2(a)]. A C-shaped n-contact partially surrounding the p-contact region [not shown in Fig. 2(a)] was formed by reactive ion etching using $SiCl_4$ into the n-region and contacted by 30/90 nm of Ti/Au and was placed $\approx$2 mm away from the p-contact. The device design is similar to those designed for electron emission spectroscopy (EES).[10,11] Circular transmission line measurements (CTLMs) indicated that both p- and n-contacts are Ohmic. The sheet resistance of the p-GaN was assumed uniform throughout the p-region and was determined from CTLM to be $1.99 \times 10^5 \Omega/\square$. The n-GaN has $R_S \approx 30\,\Omega/\square$, indicating that it is conductive and can be taken as equipotential across the aperture. The ideality factor was extracted from the current–voltage curves after removing voltage contribution due to contact resistances and was determined to be 2.015.

The diode was cleaned using a HCl:isopropanol solution to remove native oxides and dried with N_2 prior to introduction into the LEEM.[12,13] The treatment has been found to remove surface oxygen effectively at the cost of having Cl adsorption instead, tying up the dangling bonds and hindering reoxidation.[12,13] Unlike standard LEEM practice, no flash anneal or high temperature cleaning *in vacuo* was performed, as such procedures were found to degrade the p-contact. Cs was deposited on the diode surface using a SAES Getters Cs source. In LEEM, the electron landing energy on the sample, E_0, can be adjusted applying a potential of $(-20\,\text{kV} + V_0)$ to the sample, where V_0 is the start voltage as depicted in Fig. 2(b), thus decelerating the electrons that leave the objective lens from kinetic energy of 20 keV to energies close to zero.[14] As V_0 is increased, we transition from mirror mode ($E_0 < 0$) where all electrons are reflected before reaching the surface, to LEEM mode ($E_0 > 0$), where they interact with the material.[14] This mirror-mode transition (MMT) is accompanied by a sharp drop in reflected electron intensity with increasing V_0, and the inflection point of this drop identifies the vacuum level and, hence, the work function of the probed surface.[14] Work function measurement of the exposed p-GaN in the circular aperture confirmed that the vacuum level was lowered to below bulk conduction band minimum at 2.1 eV above the Fermi level. Details of the work function measurements can be found in the supplementary material (see also Ref. 15 therein).

When the diode is turned on, electrons injected from the external circuit into the n-GaN will flow across the UID-region and into the p-region, where they undergo drift-diffusion (DD) transport and

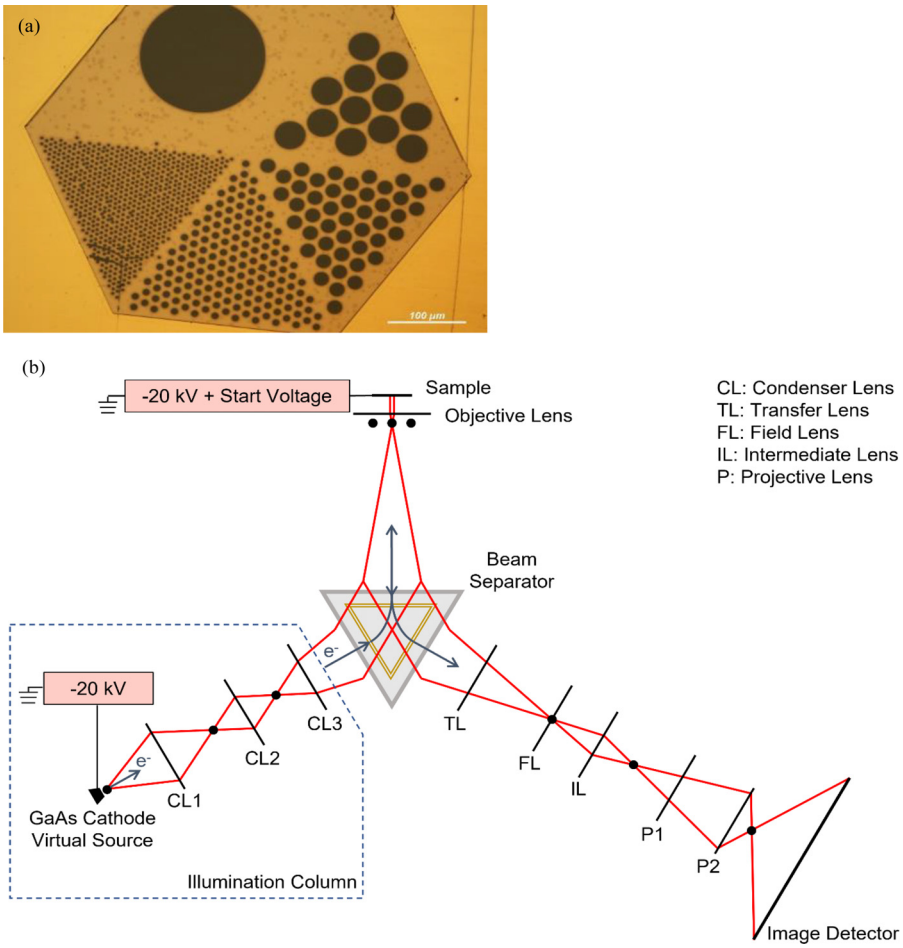

FIG. 2. (a) Optical micrograph of the device fabricated, showing the hexagonal shaped p-contact with multiple circular open apertures of various radii. (b) Schematic of the LEEM tool—with illumination column, sample chamber, and imaging column depicted. In EEM mode, the illumination column is not used.

recombination. Electrons that survived to the *p*-metal contact will exit into the external circuit, while a fraction of those reaching the surface of the vacuum-exposed *p*-GaN will be emitted provided that negative electron affinity (NEA) is achieved. The emission intensity is expected to decrease exponentially with increasing energy barrier; hence, NEA is a necessary requirement for measurement of overflow electrons.[16] In a simplistic diode model, we assume that the minority electron density in the *p*-region does not modify the Joyce–Wemple computation relying on majority hole current, and similarly the small voltage changes along the aperture do not impact electron diffusion toward the surface across the very thin p-layer compared to the much wider aperture. The emitted electron density $J_n(r)$ (density of emitted electrons measured per pixel per unit time) will scale linearly with the junction current density $J(r)$ after correction with an efficiency factor $\eta_{imaging}$ to account for losses in the imaging column. We can then write Eq. (6) in the context of this experiment as

$$J_n(r) = \eta_{imaging} J_{metal} \left(1 - \frac{I_{aper}\beta R_S}{8\pi}\left[1 - \frac{r^2}{r_{metal}^2}\right]\right)^{-2}. \quad (9)$$

The emitted electron density as a function of position was mapped using EEM in the LEEM, i.e., the GaAs cathode was turned off, so there were no electrons from the illumination column [Fig. 2(b)] incident on the diode and only electrons emitted from the diode were imaged.[17]

LEEM image of the diode indicated that the surface was satisfactorily clean from residual organic impurities, with the aperture appearing as a uniform and sharp surface in Fig. 3(a). The electron landing energy for Fig. 3(a) is −0.20 eV, which is just below the MMT, and the sample is just barely out of focus with the intent to maximize contrast while maintaining the sharpness of image features. Using image recognition to obtain the radius of the circular aperture image, the source length per pixel is found to be 0.207 μm. One observes narrow bright and dark rings near the metal edge in Fig. 3(a): It is possible that they are due to the 30 nm physical height difference between the metal contact and the GaN surface or due to the work function differences between the metal contact and the GaN surface.[14] There is a small asymmetry in the shadow at the aperture edge in Fig. 3(a), which may be due to a very slight tilt misalignment. The LEEM intensity is also uniform in the aperture, implying that the tilt of the sample must be within $\pm 0.2°$, beyond which a gradient in intensity is expected in the direction of the tilt. Since the LEEM and EEM images in Fig. 3 were measured with the same tilt alignment, such a small misalignment will not affect asymmetry in EEM electrons at $>20\,\mu$m away.

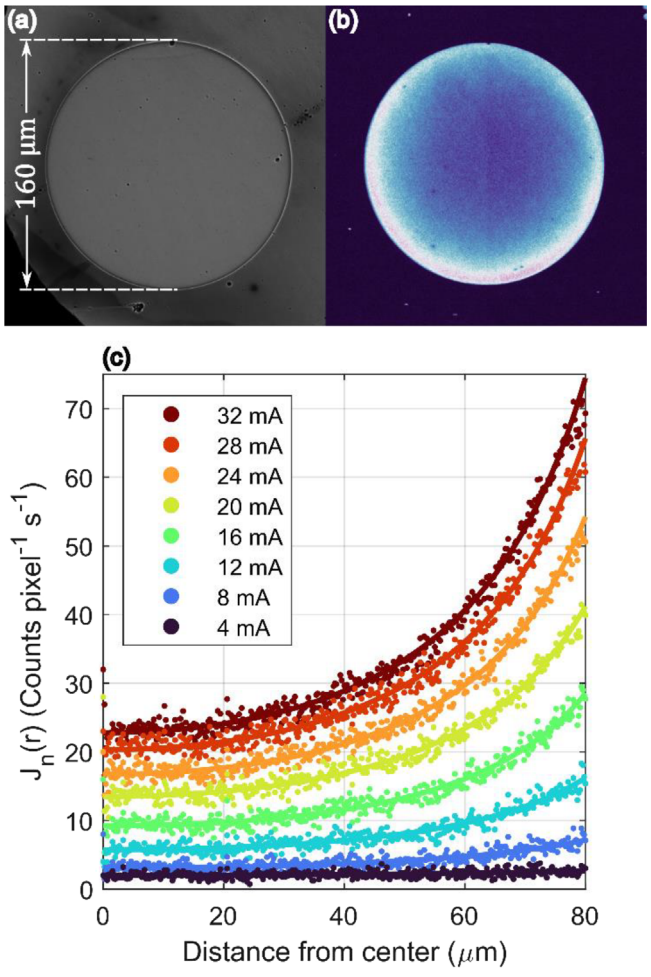

FIG. 3. (a) LEEM image of the circular aperture at zero diode bias prior to cessation. The electron landing energy is −0.20 eV, and the sample is close to in focus. (b) The emitted electron intensity profile at diode current of 32 mA. The emitted electron intensity is clearly larger near the contact metal outer edges and decreases toward the center of the aperture. The contact metal does not emit electrons. (c) The emitted electron intensities at various diode currents plotted (solid circles) fitted to Eq. (9) (solid lines), showing good agreement between data and the analytical solutions by Joyce and Wemple.[1]

The EEM image of the diode at 32 mA is shown in Fig. 3(b). As expected, the emitted electron intensity is larger near the metal contact and decreases toward the center of the circular aperture. The *p*-metal did not emit electrons, corresponding to the dark outer regions in Fig. 3(b).

The average radial emitted electron intensities for diode currents from 4 to 32 mA were obtained and fitted using non-linear least squares method to Eq. (9), as shown in Fig. 3(c). The Pearson fit coefficient to Eq. (9) was 0.99 for the intensity profile of Fig. 3(c) at diode current of 32 mA, decreasing toward 0.95 at 16 mA as measurement noise becomes more significant compared to emitted electron intensities. Additional details on the radial data analysis are included in the supplementary material. The experimental J_n is observed to be very low compared to the expected average $J = \frac{I_{diode}}{\text{Area of diode}}$, where I_{diode} is the total injected current and area of diode is the area of entire hexagonal device comprising of contacts and apertures. Nevertheless, the losses are expected to be homogeneous with respect to $J_n(r)$ and the map of the emitted current should be representative of $J(r)$. The extracted I_{aper} from the detector current measured by the image detector of the LEEM tool increases from 0.001 to 0.0062 mA for total diode current of 4 to 32 mA using $\eta = 2.015$. This huge difference is due to carrier losses in the *p*-*n* junction, loss of overflow electron from the *p*-n^- interface traveling in the *p* region toward to the surface, presence of a barrier for electron emission at the *p*-GaN surface (these three contributions measured in similar samples to lead to a ratio of emitted to injected electrons of 10^{-4}),[18] loss from the hexagonal device area due to lack of mesa confinement, the fact that there are large metal areas comprising 60% of the device, presence of numerous other smaller apertures, and losses in the imaging column. The extracted I_{aper} using Eq. (9) is functionally described by the "curvature" of the line rather than the absolute values in Fig. 3(c). Since the imaging column has constant imaging efficiency across different electron intensities,[19] one should recover I_{aper} reasonably regardless of the small measured values of electron intensities. However, carrier crowding and loss from the mesa are both non-linear losses with increasing current density and may be the reasons for the non-linear scaling of I_{aper} with increasing diode current. An estimation of the current crowding effect on I_{aper} based on the Joyce and Wemple model is included in the supplementary material.

A comparison of the goodness of fit between Joyce and Wemple model to the lateral device model showed that at low current densities, both models fit sufficiently well, while there is small discrepancy between the data and the lateral device model at high current densities, as shown in Fig. 4. This discrepancy was also demonstrated in the work of Meriggi *et al.*, which employed a square *p*-metal grid contact

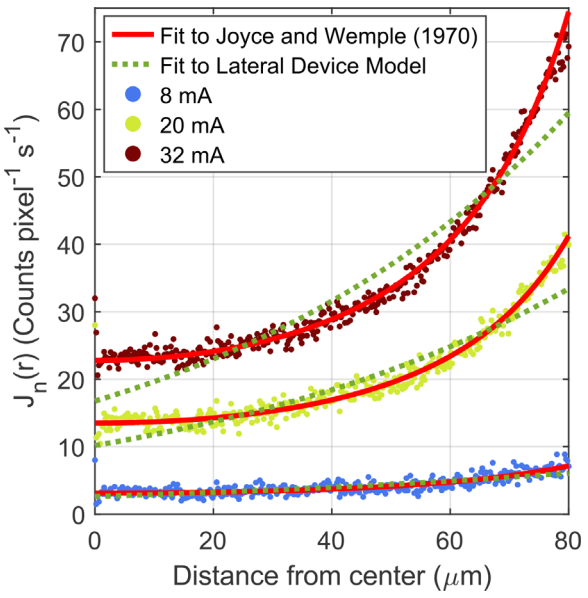

FIG. 4. Comparison of Joyce and Wemple model against lateral device model for the work described. While the overall Pearson's coefficient for the fit to the lateral device model is good, it is clearly less suitable compared to the fit provided by Joyce and Wemple model at higher current densities.

surrounding by a larger *n*-contact on the *other side* of the exposed *p*-semiconductor, similar to this work.[5] As such, the lateral device model is not suitable for describing the lateral current profile of the circular apertures described in this work.

The experimental verification of the steady-state lateral junction current profile not only has significance for laser and LED designs discussed in great length elsewhere[2–6,20] but also can be extended to previously published results on EES. In EES, the intensities and energy distributions of the emitted electrons through apertures from biased LEDs were quantitatively correlated with the efficiency drop of the LEDs.[10,11,21–25] In these (EES) experiments, small hexagonal apertures of long diagonals of 5 or 7 μm (apothems of 2.5 or 3.5 μm) were used instead of the circular aperture measured in this experiment, with the 0.22 mm^2 *p*-contact being formed from a honeycomb array of 4602 (or 2257) open apertures. However, while we obtained here clear measurements especially at higher current densities for the large aperture with radius of 80 μm, there was a lack of measurement on small apertures due to compromised surfaces from organic residues. Despite this lack of measurements on small apertures, the measurement obtained for the large aperture verified the analytical solutions, which can then be extended to describe the smaller apertures for the EES experiment.

In this demonstration of EEM imaging, we verified the functional form the analytical solutions provided by Joyce and Wemple for current through a circular aperture.[1] A future experiment with quantitative verification can be performed with a mesa isolated structure and measurements of sample emission quantum efficiency, which is beyond the scope of this demonstration.

See the supplementary material for additional details on the experiment and data analysis, which includes discussions on work function calibration using Ir (111), effects of sample tilt, and nonlinearity losses from the aperture.

Support at UCSB was provided by the Solid State Lighting and Energy Electronics Center (SSLEEC); the University of California, Santa Barbara (UCSB) – Collaborative Research of Engineering, Science and Technology (CREST) program; U.S. Department of Energy under the Office of Energy Efficiency & Renewable Energy (EERE) Award No. DE-EE0009691; the Simons Foundation (Grant Nos. 601952 and 1027114 for JSS and CW, respectively); the National Science Foundation (NSF) RAISE program (Grant No. DMS-1839077 for JSS and CW); and Sandia National Laboratory (Award No. 2150283). Work at the Molecular Foundry was supported by the Office of Science, Office of Basic Energy Sciences, of the U.S. Department of Energy under Contract No. DE-AC02-05CH11231. A portion of this work was performed at the UCSB Nanofabrication facility. Part of the results in this work make use of the colormaps in the CMasher package.

AUTHOR DECLARATIONS

Conflict of Interest

The authors have no conflicts to disclose.

Author Contributions

Wan Ying Ho: Conceptualization (equal); Formal analysis (lead); Investigation (equal); Methodology (lead); Writing – original draft (lead). **James S. Speck:** Conceptualization (equal); Formal analysis (equal); Funding acquisition (equal); Methodology (equal); Project administration (equal); Supervision (lead); Writing – review & editing (equal). **Cameron Warren Johnson:** Data curation (equal); Formal analysis (equal); Investigation (equal); Software (equal); Validation (equal); Visualization (equal); Writing – review & editing (supporting). **Tanay Tak:** Conceptualization (equal); Formal analysis (supporting); Investigation (equal); Writing – review & editing (equal). **Mylène Sauty:** Conceptualization (equal); Investigation (equal); Software (equal); Writing – review & editing (equal). **Yi Chao Chow:** Investigation (equal); Resources (lead); Writing – review & editing (supporting). **Shuji Nakamura:** Resources (equal). **Andreas Schmid:** Data curation (equal); Investigation (supporting); Supervision (supporting); Validation (equal). **Jacques Peretti:** Conceptualization (equal); Formal analysis (equal); Project administration (equal); Supervision (equal); Writing – review & editing (equal). **Claude Weisbuch:** Conceptualization (equal); Formal analysis (equal); Funding acquisition (equal); Project administration (equal); Supervision (equal); Writing – review & editing (equal).

DATA AVAILABILITY

The data that support the findings of this study are available from the corresponding author upon reasonable request.

REFERENCES

[1]W. B. Joyce and S. H. Wemple, "Steady-state junction-current distributions in thin resistive films on semiconductor junctions (Solutions of $\delta^2{}_v = \pm e^v$)," J. Appl. Phys. **41**(9), 3818–3830 (1970).
[2]X. Guo and E. F. Schubert, "Current crowding and optical saturation effects in GaInN/GaN light-emitting diodes grown on insulating substrates," Appl. Phys. Lett. **78**(21), 3337–3339 (2001).
[3]S. Hwang and J. Shim, "A method for current spreading analysis and electrode pattern design in light-emitting diodes," IEEE Trans. Electron Devices **55**(5), 1123–1128 (2008).
[4]H. Kim and S.-N. Lee, "Theoretical considerations on current spreading in GaN-based light emitting diodes fabricated with top-emission geometry," J. Electrochem. Soc. **157**(5), H562 (2010).
[5]L. Meriggi, M. J. Steer, Y. Ding, I. G. Thayne, C. MacGregor, C. N. Ironside, and M. Sorel, "Enhanced emission from mid-infrared AlInSb light-emitting diodes with p-type contact grid geometry," J. Appl. Phys. **117**(6), 063101 (2015).
[6]V. A. Sergeev and A. M. Hodakov, "Dynamic thermoelectric model of a light-emitting structure with a current spreading layer," Semiconductors **50**(8), 1079–1084 (2016).
[7]S. H. Brewer and S. Franzen, "Optical properties of indium tin oxide and fluorine-doped tin oxide surfaces: Correlation of reflectivity, skin depth, and plasmon frequency with conductivity," J. Alloys Compd. **338**(1–2), 73–79 (2002).
[8]M. Rattier, H. Benisty, R. P. Stanley, J.-F. Carlin, R. Houdre, U. Oesterle, C. J. M. Smith, C. Weisbuch, and T. F. Krauss, "Toward ultrahigh-efficiency aluminum oxide microcavity light-emitting diodes: Guided mode extraction by photonic crystals," IEEE J. Sel. Top. Quantum Electron. **8**(2), 238–247 (2002).
[9]H.-Y. Ryu and J.-I. Shim, "Effect of current spreading on the efficiency droop of InGaN light-emitting diodes," Opt. Express **19**(4), 2886 (2011).
[10]D. J. Myers, K. Gelžinytė, W. Y. Ho, J. Iveland, L. Martinelli, J. Peretti, C. Weisbuch, and J. S. Speck, "Identification of low-energy peaks in electron emission spectroscopy of InGaN/GaN light-emitting diodes," J. Appl. Phys. **124**(5), 055703 (2018).
[11]W. Y. Ho, Y. C. Chow, D. J. Myers, F. Wu, J. Peretti, C. Weisbuch, and J. S. Speck, "Quantitative correlation of hot electron emission to Auger

recombination in the active region of c-plane blue III-N LEDs," Appl. Phys. Lett. **119**(5), 051105 (2021).
[12]S. W. King, J. P. Barnak, M. D. Bremser, K. M. Tracy, C. Ronning, R. F. Davis, and R. J. Nemanich, "Cleaning of AlN and GaN surfaces," J. Appl. Phys. **84**(9), 5248–5260 (1998).
[13]O. E. Tereshchenko, G. É. Shaibler, A. S. Yaroshevich, S. V. Shevelev, A. S. Terekhov, V. V. Lundin, E. E. Zavarin, and A. I. Besyul'kin, "Low-temperature method of cleaning p-GaN(0001) surfaces for photoemitters with effective negative electron affinity," Phys. Solid State **46**(10), 1949–1953 (2004).
[14]J. Jobst, L. M. Boers, C. Yin, J. Aarts, R. M. Tromp, and S. J. van der Molen, "Quantifying work function differences using low-energy electron microscopy: The case of mixed-terminated strontium titanate," Ultramicroscopy **200**, 43–49 (2019).
[15]R. W. Strayer, W. Mackie, and L. W. Swanson, "Work function measurements by the field emission retarding potential method," Surf. Sci. **34**(2), 225–248 (1973).
[16]J. I. Pankove and H. Schade, "Photoemission from GaN," Appl. Phys. Lett. **25**(1), 53–55 (1974).
[17]E. van der Velden, "CMasher: Scientific colormaps for making accessible, informative and 'cmashing' plots," J. Open Source Software **5**(46), 2004 (2020).
[18]W. Y. Ho, Y. C. Chow, S. Nakamura, J. Peretti, C. Weisbuch, and J. S. Speck, "Measurement of minority carrier diffusion length in p-GaN using electron emission spectroscopy (EES)," Appl. Phys. Lett. **122**(21), 212103 (2023).
[19]See www.Tvips.Com for "TVIPS - TemCam F-Series," (2022).
[20]W. B. Joyce, "Carrier transport in double-heterostructure active layers," J. Appl. Phys. **53**(11), 7235–7239 (1982).
[21]J. Iveland, L. Martinelli, J. Peretti, J. S. Speck, and C. Weisbuch, "Direct measurement of Auger electrons emitted from a semiconductor light-emitting diode under electrical injection: Identification of the dominant mechanism for efficiency droop," Phys. Rev. Lett. **110**(17), 177406 (2013).
[22]J. Iveland, M. Piccardo, L. Martinelli, J. Peretti, J. W. Choi, N. Young, S. Nakamura, J. S. Speck, and C. Weisbuch, "Origin of electrons emitted into vacuum from InGaN light emitting diodes," Appl. Phys. Lett. **105**(5), 052103 (2014).
[23]D. J. Myers, K. Gelžinytė, A. I. Alhassan, L. Martinelli, J. Peretti, S. Nakamura, C. Weisbuch, and J. S. Speck, "Direct measurement of hot-carrier generation in a semiconductor barrier heterostructure: Identification of the dominant mechanism for thermal droop," Phys. Rev. B **100**(12), 125303 (2019).
[24]D. J. Myers, A. C. Espenlaub, K. Gelzinyte, E. C. Young, L. Martinelli, J. Peretti, C. Weisbuch, and J. S. Speck, "Evidence for trap-assisted Auger recombination in MBE grown InGaN quantum wells by electron emission spectroscopy," Appl. Phys. Lett. **116**(9), 091102 (2020).
[25]W. Y. Ho, A. I. Alhassan, C. Lynsky, Y. C. Chow, D. J. Myers, S. P. DenBaars, S. Nakamura, J. Peretti, C. Weisbuch, and J. S. Speck, "Detection of hot electrons originating from an upper valley at ∼1.7 eV above the Γ valley in wurtzite GaN using electron emission spectroscopy," Phys. Rev. B **107**(3), 035303 (2023).